Available online at www.sciencedirect.com
ScienceDirect
Journal of Crystal Growth 303 (2007) 449–455
JOURNAL OF CRYSTAL GROWTH
www.elsevier.com/locate/jcrysgro

Atomistic modeling of strain distribution in self-assembled interfacial misfit dislocation (IMF) arrays in highly mismatched III–V semiconductor materials

A. Jallipalli, G. Balakrishnan, S.H. Huang, A. Khoshakhlagh, L.R. Dawson, D.L. Huffaker*

Center for High Technology Materials, University of New Mexico, 1313 Goddard SE, Albuquerque, NM 87106, USA

Received 27 February 2006; received in revised form 28 October 2006; accepted 12 December 2006
Communicated by M.S. Goorsky
Available online 30 December 2006

Abstract

We describe a mathematical model to elucidate the strain energy distribution in the atomic arrangement resulting from a periodic pure edge, 90° interfacial misfit dislocation (IMF) arrays in highly mismatched III–V semiconductors. Using molecular mechanics methods, we calculate strain energy at the atomic level by considering the stretch and bend of each bond in the system under consideration. Three highly mismatched systems InAs/GaAs ($\Delta a_o/a_o$ ~7.2%), GaSb/GaAs ($\Delta a_o/a_o$ ~7.8%) and AlSb/Si ($\Delta a_o/a_o$ ~13%) are considered. This model describes that IMF array formation is driven by strain energy minimization and demonstrates the periodicity of the misfit array that is in good agreement with experimental data using cross section high-resolution transmission electron micrograph (HR-TEM) images and also with other theoretical values.
© 2007 Elsevier B.V. All rights reserved.

Keywords: A1. Periodic interfacial misfit dislocations (IMF); A1. 90° misfit arrays; A3. Molecular beam epitaxy; B1. Alsb; B1. GaAs; B1. GaSb; B1. Si; B2. Semiconducting III–V materials

1. Introduction

The epitaxial growth of highly mismatched materials has been an important technological field for two decades. In particular, lattice-mismatched epitaxy of Sb-based materials on GaAs and Si substrates are attractive for advanced optoelectronic devices including monolithically integrated lasers [1,2], detectors [3,4], solar cells [5,6] and transistors [7,8]. Two prominent approaches to mismatched epitaxy involve either thick monolithic buffer layers or interfacial misfit dislocation (IMF) arrays [9–23]. The former growth technique involves tetragonal distortion within a critical thickness followed by misfit dislocation and often threading dislocations to alleviate strain in the bulk material [24]. Researchers often mitigate the deleterious effects by bending the vertically propagating defects along strained interfaces using compositionally graded-layers or selective area growth [25,26].

The latter approach involving IMF formation appears fundamentally different from the metamorphic approach as strain energy is immediately relieved at the interface by laterally propagating (90°) misfit dislocations confined to the epi-substrate interface [9–23]. After IMF array formation, subsequent material deposition proceeds in a strain-free layer-by-layer growth mode. Our experimental observations from cross-sectional high-resolution transmission electron micrograph (HR-TEM) images suggest that the IMF arrays exist along 110 and $1\bar{1}0$ directions in GaSb/GaAs [15] and AlSb/Si [22] systems. The goal of this paper is to describe these observations mathematically and to provide a detailed analysis of the periodic strain distribution in the IMF layer. Experimental data from Trampert et al. [11] is used as a reference for modeling InAs/GaAs system.

The IMF arrays can be formed using different growth techniques, such as, MOCVD [9,10], MBE [11–16],

*Corresponding author. Tel.: +1 505 272 7845; fax: +1 505 272 7801.
E-mail addresses: anitha@unm.edu (A. Jallipalli), huffaker@chtm.unm.edu (D.L. Huffaker).

0022-0248/$ - see front matter © 2007 Elsevier B.V. All rights reserved.
doi:10.1016/j.jcrysgro.2006.12.032

atmospheric pressure MOVPE [17] and wafer bonding [18]. The IMF arrays have been reported in several systems including GaP/Si [9], GaAs/Si [10], InAs/GaAs [11], InAs/GaP [12], GaSb/GaAs [14–18], InP/GaAs [21] and AlSb/Si [22,23] over a range of lattice-mismatched conditions ranging from $\Delta a_o/a_o = 0.4\%$ (GaP/Si) to $\Delta a_o/a_o \sim 13\%$ (AlSb/Si). To date, the IMF formation process has not been well established in the literature. Some researchers explain, on the basis of Matthews's theory that the IMF arrays form to relieve strain energy when the critical thickness is less than a single monolayer [24]. At first glance, this explanation seems logical for highly mismatched systems where $\Delta a_o/a_o > 10\%$ (AlSb/Si), but is not valid for low mismatch systems, such as GaP/Si ($\Delta a_o/a_o \sim 0.4\%$), in which the critical thickness is several hundred nanometers. Even in low mismatch systems, the IMF arrays relieve ~100% strain at the epi-substrate interface (i.e., before the critical thickness has been deposited).

2. Modeling IMF arrays

There are two equilibrium models describing critical thickness of lattice-mismatched systems. The first model by Van Der Merwe compares the energy of the composite system before and after the misfits are generated. The second model by Matthews considers forces acting on a dislocation to determine critical thickness. The concept of periodic IMF arrays was first introduced by Matthews and Blakeslee [24], which states that mismatched growth undergoes tetragonal distortion up to a critical layer thickness, beyond which it forms an array of misfit dislocations. This critical layer thickness, however, can only be calculated for low to moderate mismatch materials, $\Delta a_0/a_0 < 7\%$ and does not account for immediate IMF formation at a heteroepitaxial interface. However, Matthews's theory can be used to calculate the misfit spacing of IMF arrays as shown in Table 3. Frank and Van Der Merwe (FvdM) proposed a model based on the Frenkel and Kontorowa (FK) approach of truncated Fourier series [19] to describe the IMF formation mechanics. While based on a mechanical energy minimization principle, FvdM describes the atomic position and uniformly distributed strain energy within the framework of an entire bulk material system. Both these models assume pseudomorphic growth up to critical thickness. Thus, these models are not useful as a means for understanding periodic strain distribution at the interface where there is no pseudomorphic growth.

Kuronen et al. [20] introduced molecular mechanics (MM) to study the lattice-mismatched systems characterized by gliding dislocations, such as 30° and 60° misfits. The lattice is treated as a collection of weights connected with springs, where the weights represent the nuclei and the springs represent the bonds. Strain energy is calculated by summing the individual distorted bond energies derived using the stretch and bend equations described below. This approach is unique compared to the models described above [19,24] because it enables the calculation of strain energy based on individual atomic bonds. In the work done by Kuronen et al., strain is the driving force for 30° and 60° misfit formation and 90° dislocations are formed via conventional approach, that is by the interaction of two 60° misfits. In contrast, we observe an array of spontaneous 90° misfits that form at a heterointerface. Because of the nature of this IMF array formation it is not possible to use Kuronen's model to estimate strain in IMF arrays.

To describe the HR-TEM image results mathematically and to provide a detailed analysis of the periodic strain distribution in the IMF layer, an atomistic model, which considers atom–atom interaction and bond-energetics, is necessary. In this paper, we present a model based on MM to elucidate the strain energy distribution as a function of lattice site across the array. Our findings suggest that the IMF formation is driven by strain energy minimization. We focus on the GaSb/GaAs material system to compare and validate our theoretical results.

3. IMF arrays in GaSb on GaAs

Under specific growth conditions, GaSb deposited on GaAs (0 0 1) produces periodic 90° IMF arrays along both [1 1 0] and [1 $\bar{1}$ 0] [15]. The formation of 90° dislocations needs lowest elastic energy because of its large spacing compared to 60° misfits [18]. For that reason, 90° dislocations are energetically favorable in (0 0 1) semiconductor heterointerface compared to 60° dislocations, if the formation of 90° dislocations is unobstructed [18]. In our growth process, by observing the reflection high-energy electron diffraction (RHEED) pattern, we make sure that the formation of 90° dislocations is unobstructed as mentioned in our previous work [15]. The formation of 90° rather than 60° misfits requires balancing strain energy with adatom migration based on lattice mismatch, Sb overpressure and growth temperature for GaSb/GaAs system. Specific IMF formation conditions are discussed elsewhere [15].

Figs. 1(a) and (b) shows the GaSb/GaAs IMF array in a HR-TEM image and corresponding schematic illustrating atomic arrangement and bonding in the 100 plane around the interfacial misfit. The IMF appears as two bright spots in contrast to surrounding material to indicate strain. The HR-TEM micrograph of GaSb/GaAs sample is imaged under the bright field condition using multiple beams. Other TEM images related to GaSb/GaAs IMF array also exist in one of our publications [15], where the periodicity of the IMF array can be seen on a wide range. The bonds appear homogeneous and undistorted between misfits. The HR-TEM image provides resolution of individual lattice sites. Careful observation of the lattice shows that the misfit occurs every 14 Ga lattice sites, which is equivalent to 13 Sb lattice sites. The zinc-blende atomic arrangement seems undistorted in regions between the misfits.

We note that the ratio of lattice constants, a_f:a_s is equal to the ratio of IMF periodicity, x_s:x_f, where a_f, a_s are the

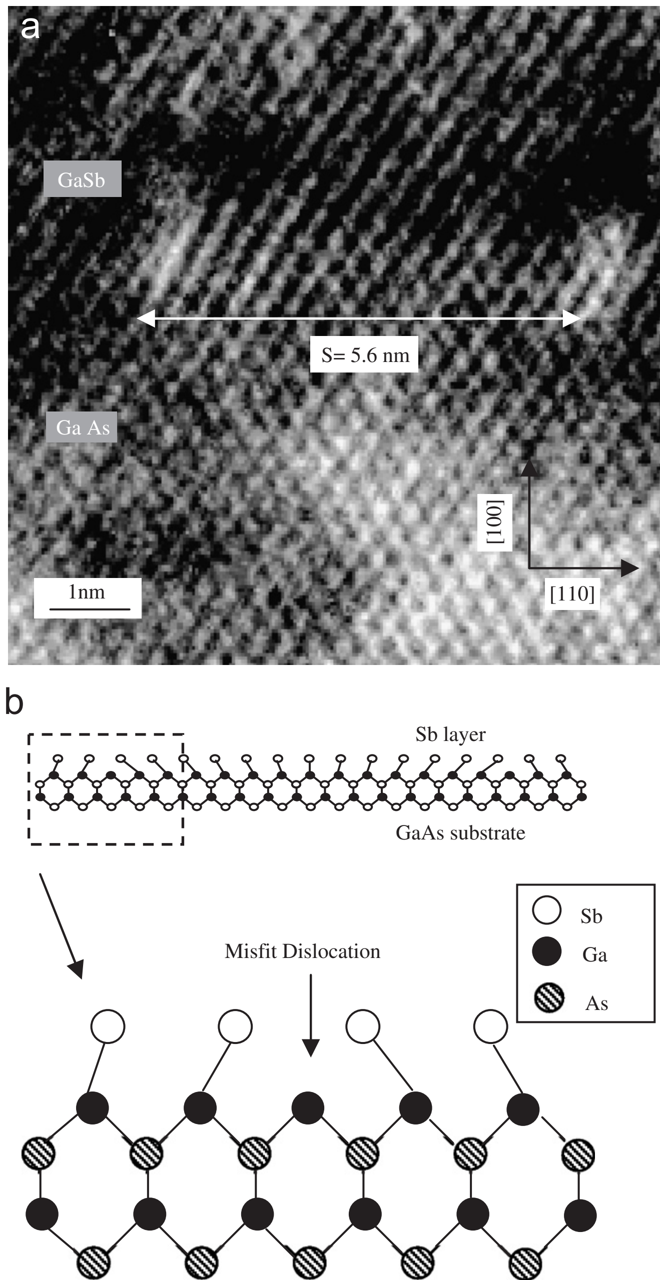

Fig. 1. (a) Cross-sectional TEM images of 120 nm GaSb bulk material on a GaAs substrate that identifies the highly periodic array of misfit dislocations at the interface of the GaSb layer and the GaAs substrate and (b) a schematic of the atomic arrangement.

lattice constants of the film and substrate and x_f, x_s are the lattice sites per IMF period in the film and substrate, respectively. The ratio x_s:x_f determines the misfit periodicity and equals 13:14 in the case of GaSb/GaAs, i.e., $x_f = 13$ lattice sites of GaSb and is equivalent in distance to 14 lattice sites in the GaAs substrate. For compressively strained material, $a_f > a_s$ and $x_s = x_f + 1$.

4. MM based calculation of interfacial strain

As described above, MM treats the lattice as a collection of weights connected with springs, where the weights represent the nuclei and the springs represent the bonds. Strain energy is calculated by summing the individual distorted bond energies derived using the stretch and bend equations described below. Electrons are not considered explicitly, but rather it is assumed that the electrons will find their optimum distribution once the positions of the nuclei are known [27]. Both the strain energy and atomic geometry at the lattice-mismatched hetero interface are derived from isolated atomic parameters such as force constants and lattice spacing.

The total strain energy for each atomic bond is expressed as the sum of several force potentials. These are E_s, energy required for stretching the atom; E_θ, energy required for bending the atoms; $E_{s-\theta}$, energy required for stretch–bend interactions; E_{tor}, torsional strain; E_{vdw}, van der Waals interactions and E_{Dp-Dp}, dipole–dipole interactions. The physical system considered in this work is sensitive primarily to two components E_s and E_θ, i.e., $E_{strain} = E_s + E_\theta$ and hence MM can also be considered as valance force field (VFF) model [28]. The VFF model was used by Musgrave and Pople [29], Keating [30] and Martin [31]. The energy required to stretch or compress an atomic bond is described using an equation similar to Hook's Law: $E_s = 143.82(K_s/2)(l - l_0)^2$, where K_s is the stretching force constant, l is the actual bond length and l_0 is the equilibrium bond length and 143.82 is a constant used to convert the stretching energy to kcal/mol. The same logic applies to bond bending as $E_\theta = 0.21914K_\theta(\theta - \theta_0)^2$ and K_θ is the bending force constant, 0.21914 is a constant used to convert the bending energy to kcal/mol, θ is the distorted bond angle and $\theta_0(=90^\circ)$ is the equilibrium bond angle. It is clear from the above equations that the distortion energy for bond stretching is directly proportional to the square of the deviation in bond length, $(l–l_0)$, where as distortion energy for bond bending is also directly proportional to the square of the deviation in bond angle, $(\theta–\theta_0)$. In our calculations, the total strain energy is in kcal/mol.

Figs. 2 illustrates the zinc-blende atomic lattice in equilibrium and distorted conditions. The figure identifies bond length, l; bond stretching, Δl; bond angle, θ; and bond bending, $\Delta\theta$. The covalent radius of Sb atom is large (1.38 Å) compared to radius of the Ga (1.26 Å) atom. Therefore, in GaSb/GaAs system, when Sb atoms are deposited on a Ga-terminated GaAs (0 0 1) surface, each Sb atom must deviate slightly from the ideal zinc-blende structure resulting in a new bond length $l + \Delta l$ and the new bond angle $\theta + \Delta\theta$ in order to accommodate the lattice and atomic size mismatch. These new bond lengths and bond angles can be very easily calculated using simple geometry based on the lattice mismatch and are different for each bond. The Ga–Sb bonds bend and stretch to accommodate the lattice mismatch. The stretching and bending continues till a physical limit is surpassed and necessitates for a skipped bond (misfit). This scenario results in a well-ordered array of periodic array of 90° misfit dislocations.

Table 1 shows peak strain energies, E_{max}, for different periodicities in GaSb/GaAs system for a grid of 17×17

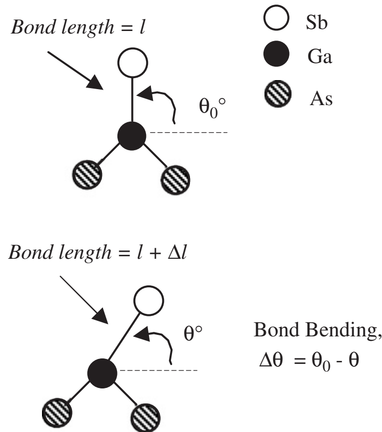

Fig. 2. Schematic drawing of undistorted and distorted lattices respectively showing l, Δl, θ, $\Delta\theta$.

Table 1
Peak strain energies E_{max} for GaSb/GaAs system for a grid of 17 × 17 atoms and shows 13:14 as the best periodicity for this system

GaSb:GaAs	E_{max} (Kcal/mol)
1:2	13726.78
2:3	3738.2
3:4	3488.08
4:5	1090.74
5:6	404.42
6:7	1225.70
7:8	964.60
8:9	335.26
9:10	273.82
10:11	219.80
11:12	172.80
12:13	132.36
13:14	105.36
14:15	141.12
15:16	183.02
16:17	231.60

atoms along [1 1 0] and [1 $\bar{1}$ 0]. We performed strain energy minimization calculations for all three systems including GaSb/GaAs, AlSb/Si and InAs/GaAs by allowing the epi (Sb in the case of GaSb/GaAs system) atoms to relax using all possible periodicities like 1:2, 2:3 and so on. This table can be used as a reference to confirm for example, why 13:14 in GaSb/GaAs system has more favorable periodicity compared to others. When the Sb atoms in GaSb/GaAs were allowed to relax using all possible periodicities, the amount of strain energy required for 13:14 is much smaller compared to the other periodicities. For example, strain energy needed for 1:2 is E_{max}~8498.65 kcal/mol, for 12:13 E_{max}~132.36 kcal/mol and for 14:15 E_{max}~141.12 kcal/mol along both [1 1 0] and [1 $\bar{1}$ 0]. From strain energy minimization calculations, we can say that the optimal strain energy distribution is always the same, 13:14 (105.36 kcal/mol) for GaSb/GaAs. The other two systems, i.e., AlSb/Si (8:9), InAs/GaAs (14:15) also behave in similar fashion (data is not shown here).

Figs. 3(a) and (b) plot the calculated stretching and bending energies, respectively, as a function of Ga atom position at the GaSb/GaAs interface along [1 1 0]. As shown in Fig. 3(a), without misfit the stretching energy will increase continuously, which is not the minimum strain energy available for the system, when it can reduce the energy required by missing a Ga atom at the interface. The other two systems including AlSb/Si, InAs/GaAs also behave in similar fashion, i.e., requires more energy without misfit. Data is not shown here for these two systems for brevity. The periodicity of the misfit array is obvious from the plots as the first misfit is placed at $x_s = 0$

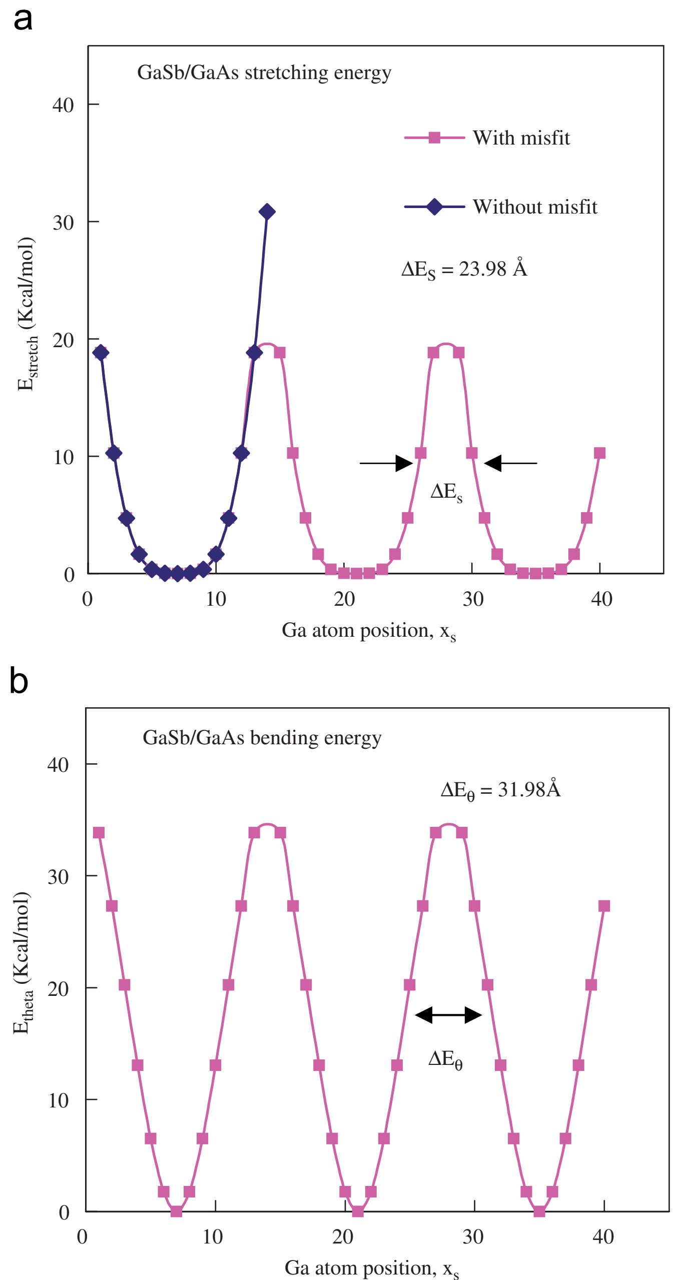

Fig. 3. (a) Stretching and (b) bending energies plotted as a function of Ga atom position at the GaSb/GaAs interface along [1 1 0].

and the subsequent misfits form every 14 Ga lattice positions (i.e. $x_s = 14$, 28, 42 and so on). From Figs. 3(a) and (b), both energy components have a maximum value around the misfit dislocation where E_s (max) ~19 kcal/mol and E_θ (max) ~34 kcal/mol. The plot also provides information about distribution of strain among the bonds as measured by full-width at half-maximum (FWHM) values. From the energy plots FWHM of GaSb/GaAs is 6 Ga atoms, i.e., 23.98 Å.

Fig. 4 is a 3D plot of total strain energy in both [1 1 0] and [1 $\bar{1}$ 0] as a function of position at the InAs/GaAs, GaSb/GaAs and AlSb/Si interfaces. A grid is formed by adding energies along both [1 1 0] and [1 $\bar{1}$ 0] to form 3D plots as shown in Fig. 4. Strain energies along both [1 1 0] and [1 $\bar{1}$ 0] are similar. The plot indicates the highly strained areas surrounding the misfits and unstrained areas between misfits using color. The color variation from blue to red shows strain energy variation from very low to very high. The peak strain energy value for InAs/GaAs, $E_{max} = 131.10$ kcal/mol, for GaSb/GaAs $E_{max} = 105.36$ kcal/mol and for AlSb/Si, $E_{max} = 335.68$ kcal/mol. The rest of the matrix experiences a strain value that lies in between the two. Areas of yellow and green between the misfit peaks indicate the residual strain between the misfits along [1 1 0] and [1 $\bar{1}$ 0]. The integrated strain energy relationship of these three systems follows the relationship of lattice mismatch, i.e., AlSb > GaSb~InAs (0.43 kcal/cm^2 > 0.20 kcal/cm^2 ~0.19 kcal/cm^2).

Table 2 shows several parameters associated with the strain energies of IMF arrays in InAs/GaAs, GaSb/GaAs and AlSb/Si. Table 2 is used for the convenience of comparing values in different material systems. The table includes lattice mismatch, bending and stretching force constants, K_s and K_θ, lattice ratios, x_f:x_s, peak strain energy, E_{max}, FWHM, maximum bond length deviation, Δl_{max}, and maximum bond angle deviation, $\Delta\theta_{max}$. Values for K_s, K_θ are tabulated in Ref. [32], while remaining constants are calculated for each material system. The lattice mismatch 7.2% and 7.8% for the InAs/GaAs and GaSb/GaAs systems and 13% for the AlSb/Si correspond to lattice ratios of 14:15, 13:14 and 8:9, respectively. The values for K_s and K_θ, which represent the amount of energy stored in the distorted bond, are rather similar for these materials: K_s ranges from 32 to 36 N/m and K_θ ~6 N/m.

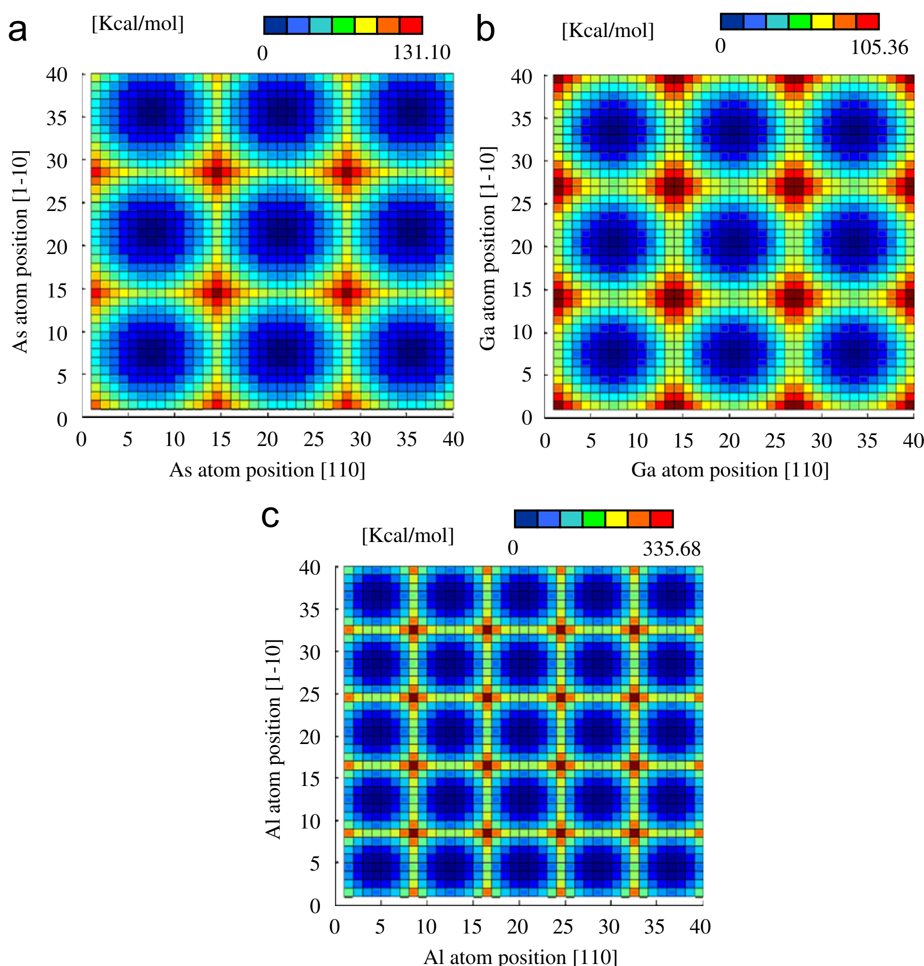

Fig. 4. 3D plots of total energy calculated at the (a) InAs/GaAs (b) GaSb/GaAs and (c) AlSb/Si interfaces using molecular modeling for a grid of 40 × 40 atoms.

Table 2
Material and calculated parameters associated with misfit arrays in the InAs/GaAs, GaSb/GaAs and AlSb/Si material systems

Parameters	InAs/GaAs	GaSb/GaAs	AlSb/Si
Mismatch (%)	7.2	7.8	13
Lattice ratios (x_s:x_f)	14:15	13:14	8:9
Stretching force constant, K_s (N/m)	35.64	32.72	34.15
Bending force constant, K_θ (N/m)	6.51	5.95	6.22
Peak energy, E_{max} (Kcal/mol)	131.10	105.36	335.68
FWHM (number of atoms, Å)	6 Ga; 23.98	6.2 Ga; 24.78	3 Si; 11.52
Max. bond length deviation, Δl_{max} (Å)	1.00	0.89	2.27
Max. bond angle deviation, $\Delta\theta_{max}$ (°)	52.94	50.94	54.93

Table 3
Misfit spacing, s, values calculated using both theory and experiment for systems with IMF arrays, formed using different techniques

Material system	Method	Misfit spacing, s (nm)			
		Theoretical		Experimental	
		MM	Matthews	Our group	Others
GaSb/GaAs	MBE	5.6 (13:14)	5.5	5.6 [15]	5.1–5.9 [14]
	MOVPE	N/A	N/A	N/A	5.8 [17]
AlSb/Si	MBE	3.47 (8:9)	3.34	3.47 [22]	3.46 [23]
InAs/GaAs	MBE	6 (14:15)	~6	N/A	8 [11]
GaAs/Si	MOCVD	N/A	9.8	N/A	7.4 [10]
InAs/GaP	MBE	N/A	3.8	N/A	4 [12]
InP/GaAs	Wafer bonding	N/A	~11	N/A	10 [21]

The table lists values for E_{max}(AlSb/Si) > E_{max}(InAs/GaAs) > E_{max}(GaSb/GaAs). The relationship E_{max}(InAs/GaAs) > E_{max}(GaSb/GaAs) is somewhat surprising considering the lattice mismatch in the two systems is just the opposite. This apparent inconsistency can be explained by considering the relative values of K_s and K_θ along with Δl_{max} and $\Delta\theta_{max}$ for InAs/GaAs and GaSb/GaAs systems, which are also important parameters in addition to lattice mismatch. The FWHM value depends on lattice constant of the substrate and the bond strength between the atoms in the substrate. For both InAs and GaSb systems, the substrate is GaAs and for AlSb, the substrate is Si. The bond strength between Si atoms will be greater compared to GaAs. For that reason, the strain energy is distributed amongst only three Si atoms compared to the other two systems, where the strain energy is distributed amongst 6 Ga atoms.

Table 3 shows both the experimental and theoretical values of different systems with IMF arrays formed by different methods. Edge dislocation spacing or misfit spacing, s, of the IMF arrays for a totally relaxed epi-layer can also be calculated theoretically using the formula [24,33] $s = b/f$, where $b = a_f/\sqrt{2}$ along [1 1 0] or [1 $\bar{1}$ 0], f is the % of lattice mismatch and is given by $f = (a_f - a_s)/a_s$, where a_s and a_f are substrate and epi-layer (film) lattice constants, respectively. The misfit periodicity calculated using MM model for AlSb/Si is 8:9 and hence is equal to the misfit spacing, $s = 8a_f = 9a_s = 3.47$ nm, where a_f and a_s are the lattice constants of the epi-layer (AlSb) and substrate (Si), respectively. Similarly, for InAs/GaAs the periodicity 14:15 is equal to $s \sim 6$ nm and for GaSb/GaAs the misfit periodicity 13:14 is equal to $s = 5.6$ nm. The misfit spacing or misfit periodicity values calculated using MM method are in good agreement with experimental HR-TEM images for InAs/GaAs [11], GaSb/GaAs [15] and AlSb/Si [22,23] as well as with Matthew's theory.

In this paper, we have plotted only the strain energy of the system. For complete understanding of the IMF formation and to claim that it is a self-assembly process, the energy of the dangling bond energy has to be considered. The MM can only calculate energy of an existing bond, not for a dangling bond. Thus, the next step in this research is to calculate the total energy of the system to find out whether IMF is a self-assembled process or an energy minimum (total energy minimum, not simply strain energy minimum) and analyzing the propagation of the strain energy into the bulk material and compare with experimental X-ray diffraction measurements.

5. Conclusion

Strain energy distribution along the periodic IMF array has been analyzed at the atomic level for several material systems including InAs/GaAs, GaSb/GaAs and AlSb/Si. Using MM, bond distortion is analyzed at the atomic level and converted to strain energy via a weighting function or

force constant. These calculations result in periodic distribution of strain energy and indicate that total strain energy is strongly dependent upon material parameters, such as stretching and bending force constant as well as lattice mismatch. Based on our calculations, the misfit array formation is driven by strain energy minimization. Calculated misfit periodicity is in good agreement with experimental HR-TEM for InAs/GaAs, GaSb/GaAs and AlSb/Si. In general, MM model can be used for any system with IMF array to calculate the misfit periodicity and to understand strain distribution in the IMF array.

References

[1] R.J. Malik, J.P. van der Ziel, B.F. Levine, C.G. Bethea, J. Walker, J. Appl. Phys. 59 (1986) 3909.
[2] J.S. Harris Jr., S.R. Bank, M.A. Wistey, H.B. Yuen, IEEE Proc. Optoelectron. 151 (2004) 407.
[3] C.G. Bethea, M.Y. Yen, B.F. Levine, K.K. Choi, A.Y. Cho, Appl. Phys. Lett. 51 (1987) 1431.
[4] L. Colace, G. Masini, F. Galluzzi, G. Assanto, G. Capellini, L. Di Gaspare, E. Palange, F. Evangelisti, Appl. Phys. Lett. 72 (1998) 3175.
[5] V.M. Andreev, O.O. Ivent'eva, E.P. Romanova, V.S. Yuferev, Sov. Phys. Tech. Phys. 28 (1983) 1242.
[6] M.L. Timmons, S.M. Bedair, R.J. Markunas, J.A. Hutchby, in: Conference Record of the Sixteenth IEEE Photovoltaic Specialists Conference-1982, 1982, p. 663.
[7] D. Lubyshev, W.K. Liu, T. Stewart, A.B. Cornfeld, J. Patton, J. Mirecki Millunchick, W. Hoke, P.F. Marsh, C. Meaton, K. Nichols, S.P. Svensson, in: Conference of the Proceedings of the International Conference on Indium Phosphide and Related Materials, 2000, p. 392.
[8] B.P. Yan, C.C. Hsu, X.Q. Wang, E.S. Yang, IEEE Electron. Device Lett. 23 (2002) 170.
[9] A.E. Blakslee, M.M. Al-Jassim, J.M. Olson, K.M. Jones, S.M. Vernon, Mater. Res. Soc. Symp. Proc. 116 (1988) 313.
[10] M.M. Al-Jassim, T. Nishioka, Y. Itoh, A. Yamamoto, M. Yamaguchi, Mater. Res. Symp. Proc. 116 (1988) 141.
[11] A. Trampert, E. Tournie, K.H. Ploog, Appl. Phys. Lett. 66 (1995) 2265.
[12] J.C.P. Chang, T.P. Chin, J.M. Woodall, Appl. Phys. Lett. 69 (1996) 981.
[13] G. Balakrishnan, S. Huang, L.R. Dawson, Y.-C. Xin, P. Conlin, D.L. Huffaker, Appl. Phys. Lett. 86 (2005) 0341051.
[14] A.M. Rocher, Solid State Phenom. 19/20 (1991) 563.
[15] S.H. Huang, G. Balakrishnan, A. Khoshakhlagh, A. Jallipalli, L.R. Dawson, D.L. Huffaker, Appl. Phys. Lett. 88 (2006) 131911.
[16] J.M. Kang, M. Nouaoura, L. Lassabatere, A. Rocher, J. Crystal Growth 143 (1994) 115.
[17] M. Aindow, T.T. Cheng, N.J. Mason, T.-Y. Seong, P.J. Walker, J. Crystal Growth 133 (1993) 168.
[18] J.M. Kang, S.-K. Min, A. Rocher, Appl. Phys. Lett. 65 (1994) 2954.
[19] J.H. Van Der Merwe, Metall. Mater. Trans. A 33A (2002) 2475.
[20] A. Kuronen, et al., Europhys. Lett. 55 (2001) 19.
[21] N.Y. Jin-Phillipp, W. Sigle, A. Black, D. Babic, J.E. Bowers, E.L. HuQuest, M. Rühle, J. Appl. Phys. 89 (2001) 1017.
[22] G. Balakrishnan, S. Huang, A. Jallipalli, L.R. Dawson, D.L. Huffaker, 48th Electronic Materials Conference, Pennsylvania State University, Pennsylvania, 2006, p. Y10.
[23] Y.H. Kim, J.Y. Lee, Y.G. Noh, M.D. Kim, S.M. Cho, Y.J. Kwon, J.E. Oh, Appl. Phys. Lett. 88 (2006) 2419071.
[24] J.W. Matthews, A.E. Blakeslee, J. Crystal Growth 27 (1974) 118.
[25] G. Balakrishnan, S. Huang, T.J. Rotter, A. Stintz, L.R. Dawson, K.J. Malloy, H. Xu, D.L. Huffaker, Appl. Phys. Lett. 84 (2004) 2058.
[26] X.Y. Sun, R. Bommena, D. Burckel, A. Frauenglass, M.N. Fairchild, S.R.J. Brueck, G.A. Garrett, M. Wraback, S.D. Hersee, J. Appl. Phys. 95 (2004) 1450.
[27] S. Teufel, Adiabatic Perturbation Theory in Quantum Dynamics, first ed, Springer, Berlin (Heidelberg/New York), 2003.
[28] J.Y. Tsao, Materials Fundamentals of Molecular Beam Epitaxy, Academic Press, Bosston, 1993, p. 95.
[29] M.J.P. Musgrave, J.A. Pople, Proc. Roy. Soc. London A 268 (1962) 474.
[30] P.N. Keating, Phys. Rev. 145 (1966) 637.
[31] R.M. Martin, Phys. Rev. B 1 (1970) 4005.
[32] V. Kumar, J. Phys. Chem. Solids 61 (2000) 91.
[33] K.-N. Tu, J.W. Mayer, L.C. Feldman, Electronic Thin Film Science for Electrical Engineers and Materials Scientists, Macmillan Publishing Company, New York, 1992, pp. 94–95,163,169.